

EVALUATING 1-G TESTING METHODS FOR PREDICTING PLANETARY ROVER MOBILITY IN REDUCED GRAVITY

Adriana Daca and Krzysztof Skonieczny

Department of Electrical and Computer Engineering, Concordia University, Montréal, Québec, Canada

ABSTRACT

Experimental apparatus and techniques for reduced gravity flight testing are being used to systematically evaluate existing Earth-based planetary rover testing methods and develop guidelines for their use and interpretation. Here, three existing testing methods for predicting wheel performance in reduced gravity are evaluated experimentally: 1) reduced-weight testing, 2) matching cone penetrometer response through soil simulant design, and 3) granular scaling laws. Based on these experiments, the granular scaling laws show great promise. The other two methods, however, did not prove to be as successful. Preparations are currently underway for further comprehensive evaluation of the latter two methods.

Key words: Planetary rovers, Mobility testing, Reduced gravity, Cone index gradient, Granular scaling laws, Parabolic flights.

1. INTRODUCTION

The world's space agencies have designated the Moon, Mars, and asteroids as priority destinations for human and robotic exploration [1]. The terrains of the Moon, Mars, and a recently discovered class of "rubble-pile" asteroids [2, 3] primarily consist of fine granular regolith dotted with rocks, the negotiation of which has proven difficult in previous exploration missions. One prime example of the extent of these difficulties is NASA's Spirit rover, which became entrenched in soft soil on Mars, ending its mission after operators were unable to free it, even with the help of many numerical and (Earth-based) experimental trials [4]. In another instance, during the Apollo 15 mission, one of the wheels of the lunar roving vehicle (LRV) became stuck, and in order to fix the problem, the astronauts had to manually move the rover to a new location [5]. This would certainly not be a feasible contingency plan in a fully robotic mission.

A fundamental understanding of wheel-soil interactions and the development of accurate rover testing methods can assist rovers in traversing difficult terrain and reaching scientifically interesting locations. Current experi-

mental predictions of rover performance are not accurate as they do not take into account the effect of reduced gravity on soil behavior. The problem of predicting soil behaviour in reduced gravity has been approached from multiple directions, for example: through soil simulant design [6, 7], through discrete element method (DEM) simulations [8], through semi-empirical modelling [9], and through scaling laws [10]. Limited experimental work has been completed; there is still a need for suitable reduced-gravity experimental data that can be used to validate approaches such as those taken in [6, 7, 8, 9, 10].

Aircraft flying parabolic arcs currently offer the best opportunity to achieve significant stretches of effectively reduced gravity in a controlled fashion without actually travelling to an extraterrestrial surface. In [11], 1/6-g, 1-g, and 2-g cone penetrometer measurements were performed aboard parabolic flights and a positive correlation between the cone index gradient (G) and gravity was observed. Reduced-gravity flights specifically measuring soil parameters including peak friction angle, residual friction angle, and angle of repose [12, 13, 14] have yet to arrive at a comprehensive consensus on how gravity affects these parameters. Additionally, reduced-gravity flights studying excavation [15] and bearing capacity [16] have similarly produced non-trivial, non-intuitive results that provide further motivation to study rover-soil interactions in reduced gravity. In [17], experimental cone penetrometer measurements were obtained under "low gravity fields" achieved using magnetic particles subjected to magnetic fields of various strengths, and a negative correlation was found between normalized tip resistance (cone index normalized by initial vertical stress) and gravity. However, these results are not validated against any actual low-gravity experimental results (e.g. from parabolic flights).

Few datasets have been described in the literature for wheels driving in soil during reduced-g flights. In a 1971 NASA report [18], a lunar roving vehicle (LRV) wheel drove along a circular path in Lunar Soil Simulant 4 (LSS-4) inside a vacuum chamber mounted inside an aircraft flying parabolic arcs, with the goal of testing fenders for dust mitigation. While the objective of these experiments was to determine the amount of dust churned up by the wheels, as well as dust settling behaviour in vacuum, low-gravity conditions, some additional interesting observations were made. Increased soil build-up

was observed in front of the wheel, which meant that more power was required to drive in lunar-g. It was also observed that vacuum conditions may have increased the apparent cohesion of the soil. Kobayashi et al. [19] performed experiments consisting of a self-propelled wheel driving in a wide range of gravity conditions. The data collected, including horizontal travel distance, vertical sinkage, and wheel torque, is contrasted to a corresponding 1-g dataset with varying wheel load. The difference between the experimental conditions in the two datasets is the effect of gravity on the soil particles themselves. Kobayashi’s key observation is that wheel travel is impaired when both the wheel and soil are in reduced gravity, rather than improving as it does when just the load on the wheel is reduced. Kobayashi’s experiment provided some evidence that adjusting the wheel loading on ground doesn’t capture the mobility performance in partial gravity. This motivated our group’s work in more comprehensively studying the effects of gravity on wheel performance, as will be presented throughout the remainder of this document.

2. BACKGROUND

2.1. Method 1: Reduced-Weight Testing

Rover mobility testing is often performed on Earth in 1-g with reduced-weight rovers or gravity offload systems to match the wheel loads the rover will experience at its destination. For example, SSTB-lite [20] and Scarecrow [21] are 3/8 mass versions of the Mars Exploration Rovers (Opportunity and Spirit) and Mars Science Laboratory rover (Curiosity), respectively, that mimic the wheel loads experienced in martian gravity. Since lunar gravity is much lower than Earth’s gravity (approximately 1/6-g), it is more difficult, but nonetheless possible and sometimes done, to use the same approach to test lunar rovers. Alternatively, lunar wheel loads can be achieved through gravity offload [22]. Although these tests correctly capture the effect of reduced gravity (and thus weight) on wheel loads, they do not capture the effect that gravity has on the granular material itself. During efforts to extricate Spirit, this may have contributed to the fact that maneuvers that were successful in on-ground (equivalent wheel load) testing did not ultimately translate into success on Mars [23].

2.2. Method 2: Equal Cone Index Gradient

A cone penetrometer is an instrument used to measure penetration resistance versus depth, giving a sense of a soil’s compaction and shear strength, and is widely used in the field of geotechnical engineering. This instrument has particular relevance to the study of soil properties in reduced gravity because in situ cone penetrometer measurements were taken during the Apollo missions to the Moon; thus, cone penetrometer measurements are usually incorporated into reduced-gravity soil studies due to

the availability of this reference data. Additionally, it has been widely used by the U.S. Army to provide a “go/no-go” assessment of terrains for off-road vehicle travel [24].

A cone penetrometer consists of a cone on a long shaft that is inserted into the ground. The pressure required for insertion (denoted cone index, CI) at a constant speed (typically about 30mm/s) is measured versus depth. A useful metric that can be derived from such data is the cone index gradient, denoted as G , calculated using Equation 1 [24]:

$$G = \frac{\sum_{i=1}^n (d_i - \bar{d})(CI_i - \overline{CI})}{\sum_{i=1}^n (d_i - \bar{d})^2} \quad (1)$$

where n is the number of measurements in an insertion, i is the measurement number, d_i and CI_i are the depth and cone index at point i , respectively, and \bar{d} and \overline{CI} are the mean of all the depth and cone index values measured in the insertion, respectively.

In [6], the lunar soil simulant GRC-1 (Glenn Research Center lunar soil simulant #1), was designed to match the in-situ cone penetrometer measurements obtained during the Apollo missions. The main assumption in the design of GRC-1 was that rover performance correlates with cone penetrometer measurements. The idea was that by preparing GRC-1 to different densities, and matching the cone penetrometer measurements to those taken during the Apollo missions to the Moon, then rovers can be more accurately tested on Earth using this new simulant. GRC-1 was designed as a frictional, cohesionless mixture of readily available manufactured sand that is prepared to a particle size distribution that is similar to the coarse fraction of lunar soil (particles $< 75\mu\text{m}$ were excluded in order to prevent dust generation). By varying the relative density of this simulant (a granular material can exist in a range of bulk densities, depending on the level of compaction), different cone index profiles can be achieved. The relative density (D_R) of a soil represents the measured bulk density of a soil relative to its minimum bulk density (0% D_R) and maximum bulk density (100% D_R). Since GRC-1 was designed to match cone index gradients (G values) from the lunar surface, it is assumed that it will also respond similarly to vehicle loading in terms of compaction and shear resistance, which control vehicle mobility [25, 26].

2.3. Method 3: Granular Scaling Laws

Granular scaling laws (GSL) are analogous to scaling relations employed in the fields of aero- and hydrodynamics that use dimensionless numbers such as the Reynold’s number. These scaling relations, recently proposed by Slonaker et al. [10], can be used to predict the performance of a larger wheel based on tests with a smaller wheel, or to predict wheel performance in one gravity level based on tests in another gravity level. The

use of scaled models to study wheels driving in loose soil, however, is by no means a new idea, and such scaling has been used in various ways since the 1950's [27, 28, 29, 30, 31, 32, 33]. Similar scaling laws for predicting reduced-gravity rover mobility had previously been derived [34, 35, 36, 37, 38] and, through slightly different means, arrived at a subset of the solutions to Slonaker's more general scaling laws. Kuroda et al. [37] performed experiments with scale-model rovers aboard parabolic flights to validate the subset of scaling laws originally proposed by Kanamori [35] in reduced gravity. Scale-model testing was also performed for the LRV program [39, 40] and has been revisited by NASA engineers in recent years [41]. The work here focuses on the version derived by Slonaker et al. [10] as it is more general than the previously derived versions. Until recently [42], the gravity-variant version of these scaling laws had only been validated through discrete element method (DEM) simulations [10, 43, 44, 45, 46]. The scaling relation that Slonaker et al. [10] derived can be seen in Equation 2. This form of the equation assumes that the wheel surface texture and the granular media are fixed for a pair of scaled tests. Then, with a standard nondimensionalization, the wheel's steady driving limit cycle is assumed to follow the form:

$$\Psi \left(\sqrt{\frac{g}{L}}t, f, \frac{g}{L\omega^2}, \frac{\rho DL^2}{M}, \frac{F_d}{Mg} \right) = \left[\frac{P}{Mg\sqrt{Lg}}, \frac{V}{\sqrt{Lg}} \right] \quad (2)$$

where Ψ is some unspecified 4-input, 2-output function, P is the power expended, M is the wheel mass, g is the gravitational acceleration, L is the characteristic length (in the case of a wheel, its radius), D is the wheel width, V is the horizontal velocity of the wheel, t is time, f is a set of points defining the wheel shape, ω is the wheel's angular velocity, ρ is the soil density, and F_d is a constant drawbar pull force. Each term in Equation 2 is dimensionless. Assuming the tests have the same wheel shape, f , and soil density, ρ , with one test having inputs $(g, L, M, D, \omega, F_d)$, and a second test having inputs $(g', L', M', D', \omega', F'_d) = (qg, rL, sM, sr^{-2}D, q^{1/2}r^{-1/2}\omega, qsF_d)$ for any positive scalars q, r , and s , each test has the same non-dimensional inputs to the function Ψ (except non-dimensional time). Then, the corresponding driving cycles are assumed to follow $\langle P' \rangle = q^{3/2}r^{1/2}s \langle P \rangle$ and $\langle V' \rangle = q^{1/2}r^{1/2} \langle V \rangle$. Recently, Zhang et al. [46] proposed a modified version of GSL that accounts for cohesion (electrostatic and/or interlocking forces between particles) and allows for sloped terrain:

$$\Psi_c \left(\sqrt{\frac{g}{L}}t, f, \frac{g}{L\omega^2}, \frac{\rho_0 DL^2}{M}, \theta, \frac{\rho_0 Lg}{\sigma_c} \right) = \left[\frac{P}{Mg\sqrt{Lg}}, \frac{V}{\sqrt{Lg}} \right] \quad (3)$$

where θ is the terrain slope angle, σ_c is cohesion stress and ρ_0 is a critical density of the granular material.

3. METHODOLOGY

3.1. Experimental setup

3.1.1. Single-wheel testbed

A specialized robotic test apparatus was previously developed to meet the constraints imposed by reduced-gravity parabolic flights [47]. In this testbed, a wheel is driven through a 90 cm \times 20 cm instrumented sandbox that collects data including drawbar pull, vertical wheel displacement (i.e. sinkage), normal force, and motor current. The wheel slip is controlled via synchronized control of a horizontal linear actuator and a wheel motor. The wheel is allowed to move freely in the vertical direction while a vertical load is applied. The testbed, shown in Figure 1 with key elements identified, also performs automated soil preparation involving loosening and compacting the soil to a repeatable state. To both enable the automatic setting of vertical wheel load and eliminate the need for bulky dead weight components, vertical wheel loading is controlled via a pair of pneumatic cylinders. Six-axis force/torque data are collected, and vertical wheel displacement is measured using a slide potentiometer. This apparatus has successfully flown aboard the Falcon 20 aircraft operated by Canada's National Research Council Flight Research Laboratory, on which various gravity conditions can be simulated for 20-25 second periods [48, 49]. Soil properties (via an automated cone penetrometer that can be attached to the test apparatus, as shown in Figure 1) can also be measured in addition to collection of wheel performance (e.g. sinkage and drawbar pull force) and video data.

3.1.2. Wheels

Two simple rigid wheels, shown in Figure 2, were 3D printed out of PLA. The large wheel has a radius of 150 mm and is 125 mm wide. The smaller wheel, used to test the granular scaling laws described in Section 2.3, has a radius of 75 mm and is 83.3 mm wide (2/3 the width of the large wheel). The selection of these dimensions is discussed further in Section 3.2.

3.2. Modification of granular scaling laws

Starting from Equation 2 in Section 2.3, the nondimensional drawbar pull term (F_d/Mg) proposed by Slonaker et al. [10] was moved to the left side of the equation, as in our experiments F_d is a measured output, not a constant input. Note that there are two methods of conducting single-wheel terramechanics experiments: controlled slip

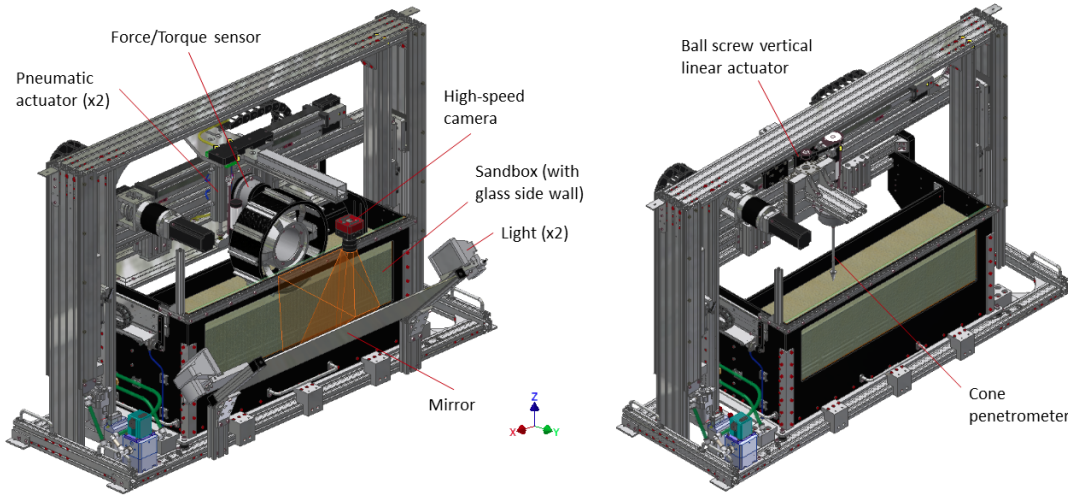


Figure 1: Design of the parabolic flight testbed with key functional elements identified, shown configured for wheel testing (left) and cone penetrometer testing (right).

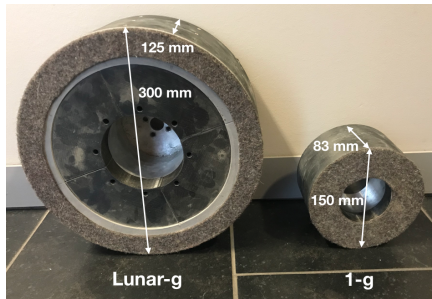


Figure 2: Large wheel used to test Method 2 in lunar-g and 1-g (left) and small wheel used to test Method 3 in 1-g (right).

(where a constant slip value is imposed) and controlled pull (where a constant drawbar pull force is applied to the wheel). While controlled pull tests more closely resemble the conditions that an actual wheel would experience, it has been shown that controlled slip tests are preferable (in terms of ease of measurement and control) for obtaining drawbar pull vs. slip curves (a standard method for characterizing wheel performance), while still generating equivalent final results [50].

Similarly, the nondimensional velocity term, V/\sqrt{Lg} , was moved to the right side of the equation, as in our experiments, the horizontal velocity is controlled in order to achieve a constant slip. Furthermore, a novel output term was added: nondimensional sinkage, z/L , as sinkage is an important output measured in these experiments. The modified function (Equation 4) is called Ω :

$$\Omega \left(\sqrt{\frac{g}{L}} t, f, \frac{g}{L\omega^2}, \frac{\rho DL^2}{M}, \frac{V}{\sqrt{Lg}} \right) = \left[\frac{F_d}{Mg}, \frac{z}{L}, \frac{P}{Mg\sqrt{Lg}} \right] \quad (4)$$

Utilizing the framework outlined in Section 3.2, with one test having inputs (g, L, M, D, ω, V) , and a second test having inputs $(g', L', M', D', \omega', V') = (qg, rL, sM, sr^{-2}D, q^{1/2}r^{-1/2}\omega, q^{1/2}r^{1/2}V)$, the scalars q , r , and s (which scale the gravity, wheel radius, and mass, respectively) can be chosen arbitrarily, and the inputs to the unspecified function Ω will remain the same for each case. For example, looking at the term $\frac{V}{\sqrt{Lg}}$ and applying the scaling factors for horizontal velocity ($V' = q^{1/2}r^{1/2}V$), gravity ($g' = qg$), and radius ($L' = rL$), the term becomes $\frac{q^{1/2}r^{1/2}V}{\sqrt{rL \cdot qg}}$, which simplifies to $\frac{V}{\sqrt{Lg}}$. In other words, $\frac{V'}{\sqrt{L'g'}} = \frac{V}{\sqrt{Lg}}$.

Correspondingly, the outputs F_d , z , and P scale such that $(F'_d, z', P') = (qsF_d, rz, q^{3/2}r^{1/2}sP)$. To evaluate the granular scaling laws experimentally, with q fixed by the relative gravity levels investigated, r and s were chosen such that the inputs and outputs fit within the operating limits of the testbed apparatus. The chosen inputs for tests in 1-g that are meant to replicate tests in lunar-g, and their corresponding outputs, can be seen in Table 1.

4. RESULTS AND DISCUSSION

Two parabolic flight campaigns have been completed to evaluate three different methods of predicting wheel performance in reduced gravity. The first parabolic flight campaign [48] was completed with the goal of evaluating the method of reduced-weight testing, and the results are summarized in Section 4.1.

The results from the second parabolic flight campaign, which evaluated the methods of matching the terrain's cone penetrometer response [49] and the use of scaling relations [42], are presented in Section 4.2.

Table 1: Inputs and outputs for the pair of scaled experiments, with $q = 6$, $r = 1/2$, and $s = 1/6$.

	Inputs					Outputs			
Lunar-g	g	L	M	D	ω	V	F_d	z	P
1-g	$6g$	$1/2 L$	$1/6 M$	$2/3 D$	3.4641ω	$1.7321V$	F_d	$1/2 z$	$1.7321P$

4.1. Method 1: Reduced-Weight Testing

Using the testbed described in Section 3.1.1, Niksirat et al. [48] compared reduced-gravity flights with on-ground experiments to evaluate the effect of reduced gravity on wheel-soil interactions of an ExoMars rover wheel prototype driving in martian soil simulant ES-2. Results from martian and lunar gravity were compared with on-ground experiments with all parameters equal, including wheel load, such that the only difference between the experiments was the effect of gravity on the soil itself (i.e. the difference between the experiments was equivalent to the difference between actually driving a rover on the Moon or Mars and testing a reduced-mass version of the rover – with equal normal wheel load – in similar soil on Earth). These experiments were the first to collect wheel-soil interaction imagery and force/torque sensor data alongside wheel sinkage data in reduced gravity. In lunar gravity, a statistically significant average reduction in traction of 20% was observed compared with 1-g, and in martian gravity an average traction reduction of 5-10% was observed. Subsurface soil imaging showed that soil mobilization increases as gravity decreases, suggesting a deterioration in soil strength, which could be the cause of the reduction in traction. Statistically significant increases in wheel sinkage in both martian and lunar gravity provided additional evidence for decreased soil strength. Thus, these experiments showed that reduced-weight mobility testing on Earth overestimates wheel performance: it overestimates drawbar pull and underestimates sinkage.

4.2. Method 2: Equal Cone Index Gradient and Method 3: Granular Scaling Laws

Using the testbed described in Section 3.1.1, the cone penetrometer response of GRC-1 was measured at three relative densities (D_R 's) in both 1-g and 1/6-g aboard parabolic flights producing effective lunar gravitational accelerations. Wheel-soil interactions between the large rigid wheel described in Section 3.1.2 and GRC-1 were also characterized at one of these densities in 1/6-g, at 20% and 70% slip. These results were compared to 1-g experiments with the same wheel in a lower-density soil that produced an equivalent cone penetrometer response, in order to test the hypothesis that equivalent wheel performance would be observed in soil with equal cone index gradients across differing gravity levels. This method of predicting wheel performance in lunar-g based on tests in 1-g will be referred to as the ‘‘Equal G method’’.

Finally, to test the expanded granular scaling laws (i.e. the ‘‘GSL method’’) described in Section 3.2, on-ground

wheel experiments were conducted using the 75 mm radius wheel and compared to the 150 mm radius wheel (see Section 3.1.2 for a description of the wheels). Comparison of the lunar-g results to the predicted drawbar pull-weight ratio (F_d/W), sinkage, and power using each method (Equal G and GSL) can be seen in Figure 3. Additionally, the mean-squared-percentage-error (MSPE) for each wheel performance metric (F_d/W , sinkage, and power) at 20% slip, 70% slip, and the average of both, using each method, can be seen in Table 2. From these figures as well as the MSPE table, the GSL method more accurately predicts wheel performance in lunar-g based on tests in 1-g. Fig. 3 shows that Equal G testing in 1-g overestimates Lunar wheel performance – it overestimates drawbar pull and underestimates sinkage, similarly to Reduced-Weight Testing. Thus, the assumption made during the creation of GRC-1 is not quite accurate, and equivalent G values did not result in equivalent wheel performance. On the other hand, it appears that the GSL method tends to err on the side of underestimating wheel performance (underestimating drawbar pull and overestimating sinkage). This indicates that the GSL method is not only more accurate, but is also a more conservative method for predicting wheel performance in reduced gravity based on tests in 1-g.

5. CONCLUSION AND FUTURE WORK

Three existing Earth-based (1-g) testing methods for predicting wheel performance in reduced gravity are evaluated in this work: 1) matching wheel loads using reduced-weight robots, 2) matching soil testing instrument (cone penetrometer) response through soil simulant design, and 3) the use of scaling relations to test scaled wheels/robots. Experimentation campaigns flying reduced-gravity parabolas aboard the National Research Council of Canada’s (NRC) Falcon 20 aircraft, with soil and wheel both in lunar-g, have shown reductions in net traction (i.e. drawbar pull) of 20% or more and increases in sinkage of up to 40% compared to Earth-based testing methods 1 and 2. Scaled-wheel testing, according to GSL (method 3) has shown better agreement with reduced-g tests (<10% error) and also tends to err on the side of conservative predictions. We are in the process of preparing a follow-on experimentation campaign utilizing a more cohesive lunar simulant to confirm and elaborate upon these findings. The ultimate near-term objective of this work is to develop guidelines for conducting and interpreting 1-g mobility tests for lunar rovers.

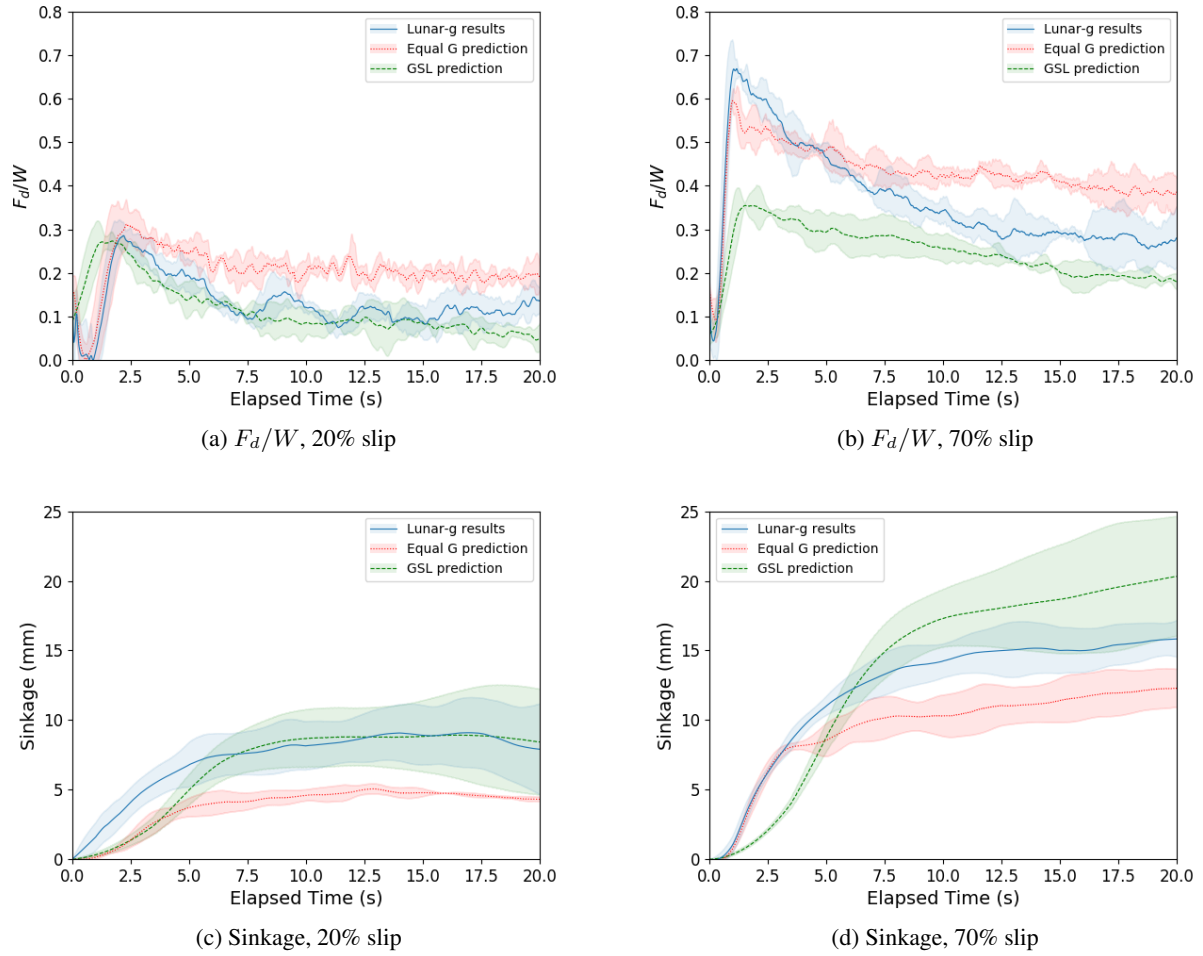


Figure 3: Drawbar pull-weight ratio (F_d/W) and sinkage measured in lunar-g compared to Equal G and GSL predictions. Each line consists of an average of three to four experimental repeats. Light-coloured regions represent 95% confidence intervals.

Table 2: Mean squared percentage error (MSPE) from 5 - 20 s.

	Method 1: Equal cone index gradient (G)			Method 2: Granular scaling laws (GSL)		
	20% slip	70% slip	Average	20% slip	70% slip	Average
F_d/W	76%	12%	44%	9%	8%	8.5%
Sinkage	21%	6%	13.5%	0.4%	5%	2.7%
Power	8%	1%	4.5%	7%	0.6%	3.8%

ACKNOWLEDGMENTS

This project was undertaken with the financial support of the Canadian Space Agency, the Natural Sciences and Engineering Research Council of Canada (NSERC), and the Fonds de Recherche du Québec - Nature et Technologies (FRQNT). The authors thank Canada's National Research Council Flight Research Laboratory, especially Derek "Duff" Gowanlock and Shahrukh Alavi, for facilitating the parabolic flight campaigns. The authors would also like to thank Pierre-Lucas Aubin-Fournier for 3D printing the rigid wheels and Dominique Tremblay for assistance with modifying the experimental apparatus and running the experiments.

REFERENCES

- [1] International Space Exploration Coordination Group. Global exploration roadmap. Technical report, National Aeronautics and Space Administration Headquarters, Washington, DC, 2018.
- [2] A. Fujiwara, J. Kawaguchi, D. Yeomans, M. Abe, T. Mukai, T. Okada, J. Saito, H. Yano, M. Yoshikawa, and D. Scheeres. The rubble-pile asteroid itokawa as observed by hayabusa. *Science*, 312:1330–1334, Jun 2006.
- [3] B. Rozitis, E. MacLennan, and J. P. Emery. Cohesive forces prevent the rotational breakup of rubble-pile asteroid (29075) 1950 da. *Nature*, 512:174, Jun 2014.
- [4] D Brown and G Webster. Now a Stationary Research Platform, NASA's Mars Rover Spirit Starts a New Chapter in Red Planet Scientific Studies. *NASA Press Release*, 2010.
- [5] Nicholas C Costes, John E Farmer, and Edwin B George. *Mobility Performance of the Lunar Roving Vehicle: Terrestrial Studies, Apollo 15 Results*, volume 401. NASA, 1972.
- [6] Heather A Oravec, Xiangwu Zeng, and Vivake M Asnani. Design and characterization of GRC-1: A soil for lunar terramechanics testing in earth-ambient conditions. *Journal of Terramechanics*, 47(6):361–377, 2010.
- [7] Michael B Edwards, Mandar M Dewoolkar, Dryver R Huston, and Colin Creager. Bevameter testing on simulat fillite for planetary rover mobility applications. *Journal of Terramechanics*, 70:13–26, 2017.
- [8] Mingjing Jiang, Fang Liu, Huaning Wang, and Xinxin Wang. Investigation of the effect of different gravity conditions on penetration mechanisms by the distinct element method. *Engineering Computations*, 32(7):2067–2099, 2015.
- [9] László L Kovács, Bahareh Ghotbi, Francisco González, Parna Niksirat, Krzysztof Skonieczny, and József Kövecses. Effect of gravity in wheel/terrain interaction models. *Journal of Field Robotics*, 2019 (In Press).
- [10] James Slonaker, D Carrington Motley, Qiong Zhang, Stephen Townsend, Carmine Senatore, Karl Iagnemma, and Ken Kamrin. General scaling relations for locomotion in granular media. *Physical Review E*, 95(5):052901, 2017.
- [11] NC Costes, GT Cohron, and DC Moss. Cone penetration resistance test-an approach to evaluating in-place strength and packing characteristics of lunar soils. In *Lunar and Planetary Science Conference Proceedings*, volume 2, page 1973, 1971.
- [12] Khalid A Alshibli, Susan N Batiste, and Stein Sture. Strain localization in sand: plane strain versus triaxial compression. *Journal of Geotechnical and Geoenvironmental Engineering*, 129(6):483–494, 2003.
- [13] MG Kleinhans, H Markies, SJ De Vet, and FN Postema. Static and dynamic angles of repose in loose granular materials under reduced gravity. *Journal of Geophysical Research: Planets*, 116(E11), 2011.
- [14] Jason P Marshall, Ryan C Hurley, Dan Arthur, Ivan Vlahinic, Carmine Senatore, Karl Iagnemma, Brian Trease, and José E Andrade. Failures in sand in reduced gravity environments. *Journal of the Mechanics and Physics of Solids*, 113:1–12, 2018.
- [15] W.W. Boles, W. D. Scott, and J. F. Connolly. Excavation forces in reduced gravity environment. *Journal of Aerospace Engineering*, 10:99–103, 1997.
- [16] H. H. Bui, T. Kobayashi, R. Fukagawa, and J. C. Wells. Numerical and experimental studies of gravity effect on the mechanism of lunar excavations. *Journal of Terramechanics*, 46:115–124, 2009.
- [17] Pin-Qiang Mo, Feng Gao, Guoqing Zhou, Ruilin Li, Kang Yan, and Jun Chen. An experimental study on triaxial compression tests and cone penetration tests in planetary regolith simulat under low gravity fields. *Journal of Testing and Evaluation*, 47(3):1677–1700, 2018.
- [18] C Howell Mullis. A study and analysis of the MSFC lunar roving vehicle dust profile test program. Technical Report NASA CR-121075, NASA, 1971.
- [19] T. Kobayashi, Y. Fujiwara, J. Yamakawa, N. Yasufuku, and K. Omine. Mobility performance of a rigid wheel in low gravity environments. *Journal of Terramechanics*, 47:261–274, 2010.
- [20] Joseph Carsten, Arturo Rankin, Dave Ferguson, and Anthony Stentz. Global planning on the mars exploration rovers: Software integration and surface testing. *Journal of Field Robotics*, 26(4):337–357, 2009.
- [21] Matt Heverly, Jaret Matthews, Justin Lin, Dan Fuller, Mark Maimone, Jeffrey Biesiadecki, and John Leichty. Traverse performance characterization for the mars science laboratory rover. *Journal of Field Robotics*, 30(6):835–846, 2013.
- [22] Krzysztof Skonieczny, D S Wettergreen, and W L Whittaker. Advantages of continuous excavation in

- lightweight planetary robotic operations. *The International Journal of Robotics Research*, 35(9):1121–1139, 2016.
- [23] John L Callas. Mars Exploration Rover Spirit End of Mission Report. Technical Report JPL D-92756, NASA, 2015.
- [24] JL McRae, CJ Powell, and RD Wismer. Performance of soils under tire loads, report 1: test facilities and techniques. *U.S. Army Engineer Waterways Experiment Station*, 1965.
- [25] MG Bekker. Land locomotion on the surface of planets. *ARS journal*, 32(11):1651–1659, 1962.
- [26] Mieczyslaw Gregory Bekker. Mechanics of locomotion and lunar surface vehicle concepts. *Sae Transactions*, pages 549–569, 1964.
- [27] M. G. Bekker. *Theory of land locomotion*. University of Michigan Press, Ann Arbor, 1956.
- [28] RJ Sullivan. Earthmoving in miniature. *Journal of Terramechanics*, 1(4):85–106, 1964.
- [29] Dean R Freitag et al. *A dimensional analysis of the performance of pneumatic tires on soft soils*, volume 3. Auburn University., 1965.
- [30] Robert Louis Schafer. *Model-prototype studies of tillage implements*. PhD thesis, 1965.
- [31] A Soltynski. Physical similarity and scale effects in soil-machine systems. *Journal of Terramechanics*, 5(2):31–43, 1968.
- [32] Dean Richard Freitag, Robert L Schafer, and Robert D Wismer. Similitude studies of soil-machine systems. *Journal of Terramechanics*, 7(2):25–58, 1970.
- [33] RD Wismer, DR Freitag, and RL Schafer. Application of similitude to soil-machine systems. *Journal of Terramechanics*, 13(3):153–182, 1976.
- [34] D Schuring. Scale model testing of land vehicles in a simulated low gravity field. *SAE Transactions*, 75:699–705, 1967.
- [35] Hiroshi Kanamori. Terramechanics in lunar and planetary exploration. *Journal of the Robotics Society of Japan*, 21(5):480–483, 2003 (In Japanese).
- [36] Yoji Kuroda, Teppei Teshima, Yoshinori Sato, and Takashi Kubota. Mobility performance evaluation of planetary rover with similarity model experiment. In *IEEE International Conference on Robotics and Automation, 2004. Proceedings. ICRA'04. 2004*, volume 2, pages 2098–2103. IEEE, 2004.
- [37] Yoji Kuroda, Teppei Teshima, Yoshinori Sato, and Takashi Kubota. Mobility performance evaluation of planetary rovers in consideration of different gravitational acceleration. In *2005 IEEE/RSJ International Conference on Intelligent Robots and Systems*, pages 2991–2996. IEEE, 2005.
- [38] Meng Li, Feng Gao, and Peng Sun. Prediction method of lunar rover’s tractive performance based on similitude methodology. In *Fifth International Conference on Intelligent Computation Technology and Automation*, pages 686–689. IEEE, 2012.
- [39] EG Markow. Predicted behavior of lunar vehicles with metalastic wheels. *SAE Transactions*, 72:388–396, 1964.
- [40] Allen S Lessem. Operations and maintenance manual for a scale-model lunar roving vehicle. Technical report, U.S. Army Engineer Waterways Experiment Station, 1972.
- [41] Kyle Johnson, Vivake Asnani, Jeff Polack, and Mark Plant. Experimental evaluation of the scale model method to simulate lunar vehicle dynamics. In *International Society for Terrain-Vehicle Systems (ISTVS) Americas Regional Conference*, 2016.
- [42] Adriana Daca, Dominique Tremblay, and Krzysztof Skonieczny. Expansion and experimental evaluation of scaling relations for the prediction of wheel performance in reduced gravity. *In Preparation*, 2022.
- [43] Andrew Thoesen, Teresa McBryan, and Hamidreza Marvi. Helically-driven granular mobility and gravity-variant scaling relations. *RSC advances*, 9(22):12572–12579, 2019.
- [44] Andrew Thoesen, Teresa McBryan, Darwin Mick, Marko Green, Justin Martia, and Hamid Marvi. Comparative performance of granular scaling laws for lightweight grouser wheels in sand and lunar simulant. *Powder Technology*, 373:336–346, 2020.
- [45] Andrew Thoesen, Teresa McBryan, Darwin Mick, Marko Green, Justin Martia, and Hamid Marvi. Granular scaling laws for helically driven dynamics. *Physical Review E*, 102(3):032902, 2020.
- [46] Qiong Zhang, Stephen Townsend, and Ken Kamrin. Expanded scaling relations for locomotion in sloped or cohesive granular beds. *Physical Review Fluids*, 5(11):114301, 2020.
- [47] Krzysztof Skonieczny, Parna Niksirat, and Amir Ali Forough Nassiraei. Rapid automated soil preparation for testing planetary rover-soil interactions aboard reduced-gravity aircraft. *Journal of Terramechanics*, 83:35–44, 2019.
- [48] Parna Niksirat, Adriana Daca, and Krzysztof Skonieczny. The effects of reduced-gravity on planetary rover mobility. *International Journal of Robotics Research*, 39(7):797–811, 2020.
- [49] Adriana Daca, Dominique Tremblay, and Krzysztof Skonieczny. Experimental evaluation of cone index gradient as a metric for the prediction of wheel performance in reduced gravity. *Journal of Terramechanics*, 99:1–16, 2022.
- [50] N.R. Murphy and A.J. Green. Effects of test techniques on wheel performance. *Journal of Terramechanics*, 6(1):37 – 52, 1969.